TECHNICAL REPORT BRL-TR-3148

BRL

THERMAL RADIATION SIMULATOR CHARACTERIZATION METHODS FOR THE RECTANGULAR PULSE

RICHARD B. LOUCKS

SEPTEMBER 1990

U.S. ARMY LABORATORY COMMAND

BALLISTIC RESEARCH LABORATORY
ABERDEEN PROVING GROUND, MARYLAND

NOTICES

Destroy this report when it is no longer needed. DO NOT return it to the originator.

Additional copies of this report may be obtained from the National Technical Information Service, U.S. Department of Commerce, 5285 Port Royal Road, Springfield, VA 22161.

The findings of this report are not to be construed as an official Department of the Army position, unless so designated by other authorized documents.

The use of trade names or manufacturers' names in this report does not constitute indorsement of any commercial product.

REPORT DOCUMENT PAGE

Form Approved
OMB No. 0704-0188

1. AGENCY USE ONLY *(Leave blank)*	2. REPORT DATE	3. REPORT TYPE AND DATES COVERED
	September 1990	Final, Jan 90 - Jul 90

4. TITLE AND SUBTITLE
Thermal Radiation Simulator Characterization Methods for the Rectangular Pulse

5. FUNDING NUMBERS
1L1612120AH25

6. AUTHOR(S)
Richard B. Loucks

7. PERFORMING ORGANIZATION NAME(S) AND ADDRESS(ES)
Director
U.S. Army Ballistic Research Laboratory
ATTN: SLCBR-TB-BD
Aberdeen Proving Ground, MD 21005-5066

8. PERFORMING ORGANIZATION REPORT NUMBER

9. SPONSORING/MONITORING AGENCY NAMES(S) AND ADDRESS(ES)
U.S. Army Ballistic Research Laboratory
ATTN: SLCBR-DD-T
Aberdeen Proving Ground, MD 21005-5066

10.SPONSORING/MONITORING AGENCY REPORT NUMBER
BRL-TR-3148

11. SUPPLEMENTARY NOTES

12a. DISTRIBUTION/AVAILABILITY STATEMENT
Approved for public release; distribution is unlimited.

12b. DISTRIBUTION CODE

13. ABSTRACT *(Maximum 200 words)*

Thermal radiation simulation of nuclear events have been achieved by a variety of processes due to the ban on above ground nuclear tests. Each thermal radiation simulator is unique in its ability and limitations. The simulator type addressed within is the liquid oxygen/aluminum powder combustion Thermal Radiation Simulator (TRS), used by the Blast Dynamics Branch at the Ballistic Research Laboratory, Maryland, the Thermal Radiation Source Test Facility at Kirtland AFB, New Mexico, and the Centre d'Etude in Gramat, France.

Where a square thermal pulse is desired, the ensuing flux vs. time record is ordinarily a rough approximation. Time delays brought on by valve actuations and turbulence in the flame wall all serve to distort the desired perfect rectangular pulse. The result is to generate disagreement as to what the actual average flux level is and the length of pulse duration. Four different analytical schemes to determine average flux and pulse duration are presented and compared. Advantages and restrictions are discussed.

14. SUBJECT TERMS
Nuclear Explosion Simulation, Thermal Radiation, Heat Transfer, Heat Conductivity, Thermal Conductivity, Numerical Analysis, Finite Difference Theory.

15. NUMBER OF PAGES
44

16. PRICE CODE

17. SECURITY CLASSIFICATION OF REPORT	18. SECURITY CLASSIFICATION OF THIS PAGE	19. SECURITY CLASSIFICATION OF ABSTRACT	20. LIMITATION OF ABSTRACT
UNCLASSIFIED	UNCLASSIFIED	UNCLASSIFIED	UNLIMITED

INTENTIONALLY LEFT BLANK.

Acknowledgements

The author wishes to express his gratitude to Mr. Gerald Bulmash and Mr. Peter Muller for their support and guidance. Their helpful assistance paved the way for the basis of this report. Special thanks go to Mr. Richard Thane for continuous technical support in generating the data available.

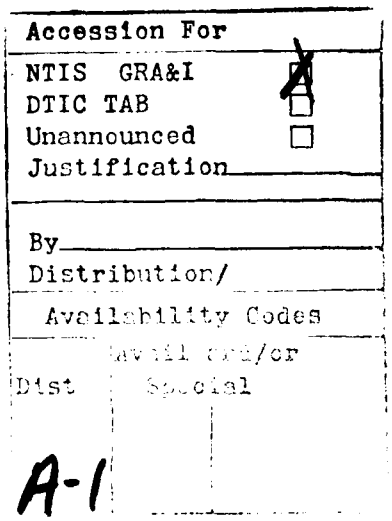

INTENTIONALLY LEFT BLANK.

Table of Contents

		Page
	Acknowledgements	iii
	List of Figures	vii
	List of Tables	ix
1.	Introduction	1
2.	Thermal Radiation Simulators	1
3.	Data Analysis Schemes	2
	3.1 Full Width Method	2
	3.2 Full Width at Half Maximum Method	3
	3.3 Moments Matching Method	4
	3.4 Fourier Averaging Method	4
4.	Simulation of a Target Response	6
	4.1 Analytical Solution	6
	4.2 Numerical Solution	8
	4.3 Target and Thermal Radiation Simulator Data	10
5.	Results of the Parameterization of the Five TRS Data Traces	12
6.	Conclusions	19
	References	21
	Appendix A	23
	Appendix B	27
	Appendix C	31
	Appendix D	35
	Distribution List	41

INTENTIONALLY LEFT BLANK.

List of Figures

Figure		Page
1	Typical TRS output of the BRL Facility, APG, MD	2
2	Comparisons between a)Flux record and b) ideal Rectangular pulse	3
3	Comparisons between TRS Data and Full Width Method	3
4	Comparisons between TRS Data and Full Width Method at Half Maximum	4
5	Fourier Transform of a Rectangular Pulse	5
6	Infinite slab considered for target response	7
7	Five U.S. BRL TRS Record Traces used for Characterization scheme comparisons.	11
8	Coordinate system used in locating calorimeter position relative to BRL TRS Nozzle.	11
9	Comparisons of the results of numerically computed temperature profiles on the target surface using Trace 1 and Trace 2 with their respective idealized thermal pulses.	14
10	Comparisons of the results of numerically computed temperature profiles on the target surface using Trace 3 and Trace 4 with their respective idealized thermal pulses.	15
11	Comparisons of the results of numerically computed temperature profiles on the target surface using Trace 5 with its respective thermal pulses.	16
12	Comparisons of the results of numerically computed temperature profiles on the target surface using Trace 4 and the respective four idealized thermal pulse taken over a) a selected range of data and b) the entire range of data.	17
13	Comparisons of the Fourier Transform of a) Trace 2 and decimated Trace 2, b) Trace 3 and decimated Trace 3.	18
14	Magnitude and Derivative of Fourier Transform of 50 $cal/cm^2 - sec$ by 1 sec pulse.	28
15	Flow Chart for determining Pulse Width	29

INTENTIONALLY LEFT BLANK.

List of Tables

Table		Page
1	Results of numerical and analytical comparisons	9
2	TRS Data Parameters as established by the Characterization Schemes. . . .	12
3	Comparisons of Characterization Schemes results between full data set and decimated data set.	13

INTENTIONALLY LEFT BLANK.

1. Introduction

Determination of the **average flux** level, or the thermally radiant intensity, and **pulse length** from an aluminum powder/ liquid oxygen Thermal Radiation Simulator (TRS) has generated debate because of the nature of TRS output and its erratic nature. A scheme is needed to quantify flux against time output into single values for TRS characterization purposes.

Past attempts to shape the thermal pulse from a TRS to match that of a nuclear weapon have not been entirely successful. The TRS rectangular pulse is the most widely used and accepted. Current technology permits such pulses to be produced with rapid rise and fall times (less than 100 msec. to full flux capacity).

The problem is how to quantify the thermal output into simple values for comparisons against other TRS performances or for predicting target response. The TRS can be programmed to turn on and off, but the thermal output is still a widely variant distortion of a rectangular pulse. Depending on the location of the heat sensing device, the variation can exceed up to 20% of the observed mean flux. Determining values for average flux and pulse time are difficult to establish with specificity.

Four schemes, for determining the average flux and pulse duration are presented. They are the 1) Full Width Method, 2) Full Width at Half Maximum Method, 3) Moments Matching Method and 4) the Fourier Averaging Method. Each method is presented with its respective advantages and limitations. The results are then compared to the predicted analytical and numerical responses of different targets. These methods all represent attempts to quantify the TRS data in a consistent manner for comparison with other TRS data.

2. Thermal Radiation Simulators

There exist at least four different methods currently used for nuclear thermal radiation simulation [1]. Solar furnaces, such as the White Sands Missile Range, New Mexico, and Centre d'Essais d'Odeillo, France, consist of a large mirror that tracks the relative movement of the sun with the earth and reflects the suns rays onto a parabolic array of concentrator mirrors . The sunlight is focused into a small area of irradiation. Because of the high flux levels achievable, and the nature of the system, nuclear event pulses may be imitated with accuracy. Unfortunately, the concentrator only irradiates a small area, and the facility cannot be used for large targets.

The Xenon Flashlamp Facility and Quartz Lamp Bank Facilities at Tri-Service Thermal Radiation Test Facility, Wright-Patterson Air Force Base, Ohio, have consistent outputs, but are limited by the amount of target area that can be exposed. The Xenon Flashlamp can simulate the nuclear pulse, but like the solar facility, can only expose a target 4 by 4 in. [1]. The Quartz Lamp Bank is similar to the TRS in that its output is also a square wave. It is plagued by a small irradiation surface, a relatively low flux output level (10 inch long by 6 inch high, 55 cal/cm^2s) and large electrical energy requirements.

The aluminum/liquid oxygen Thermal Radiation Simulator uses the latent energy released by radiation of the condensing particles of aluminum oxide [3]. The aluminum powder is jetted into the air at high velocity along with saturated liquid oxygen. The mixture passes an ignition point and combusts. This process creates a large wall of flame radiating at a high temperature. Unfortunately, the TRS flame is extremely sensitive to boundary conditions, yielding variation in the output. As shown in Figure 1, the TRS output does yield some average flux over some definite time frame.

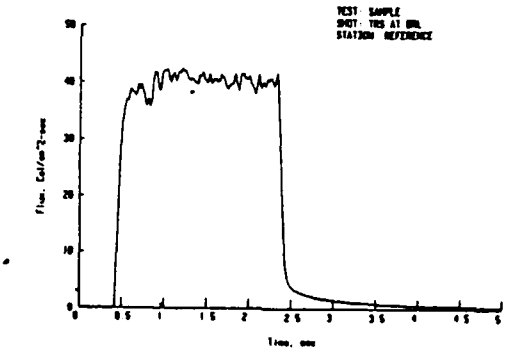

Figure 1. *Typical TRS output of the BRL Facility, APG, MD*

3. Data Analysis Schemes

The output of the Thermal Radiation Simulator is difficult to control. Regulation of the aluminum powder flow to the combustion nozzle is difficult without a sophisticated control feedback system. The BRL TRS procedure is to preset the aluminum containment vessel pressures. A valve at the bottom of the vessel opens and closes aluminum flow to the system. A valve at the combustion nozzle controls the direction of aluminum flow. Aluminum flows either to a waste recovery system or to the combustion chamber. During TRS operation, the aluminum powder is allowed to flow in the waste recovery system for a few seconds, and then diverted into the combustion chamber with minimal disturbance to the steady flow. The result is a more controlled rectangular thermal pulse. While the flux record does not match that of a nuclear pulse, the fluence is matched, effectively exposing a target to an equivalent thermal environment.

Since the TRS output is rectangular, several schemes have been developed to quantify the output as an ideal rectangular thermal pulse with defined amplitude and duration. The amplitude can be described as the average flux. The duration is the time of thermal output at the defined average flux, or pulse width.

3.1 Full Width Method

The Full Width method defines the pulse width of the flux record as the time from the initiation of the TRS, until the flux level has dropped below some minimum point close to

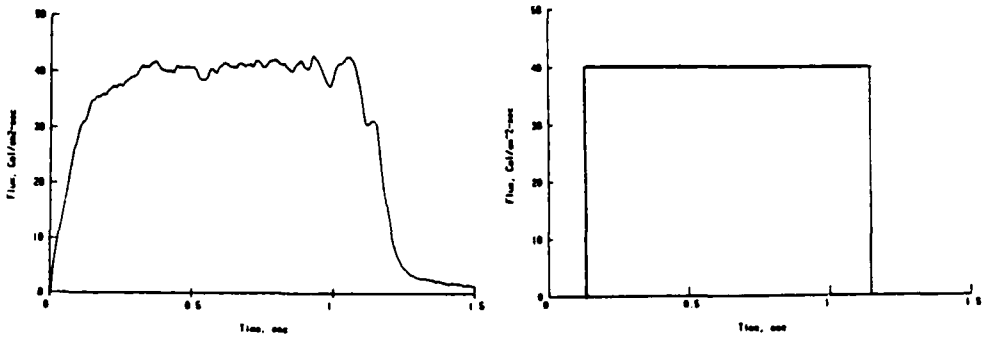

Figure 2. *Comparisons between a)Flux record and b) ideal Rectangular pulse*

the baseline. The amplitude is then determined by dividing the **fluence**, or the integrated flux record, by the pulse width. The beginning of a flux record ordinarily is well defined, but the termination point is vague due to hot cloud residue still present to the target well after shut-down. This leaves a decaying trail on the calorimeter data and prolongs the termination point. As seen in Figure 3, the determination of the pulse width usually leads to low amplitude levels, poorly characterizing the TRS data.

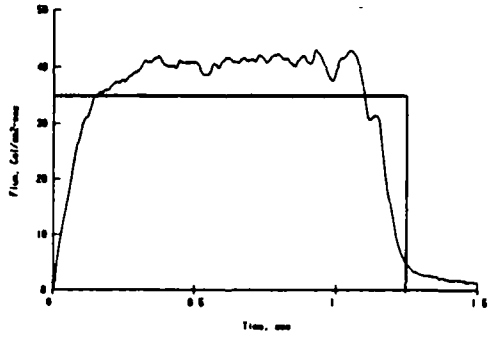

Figure 3. *Comparisons between TRS Data and Full Width Method*

3.2 Full Width at Half Maximum Method

This method is very much a corrected Full Width method. The Full Width method is modified by redefining the pulse width onset and termination points. These points are defined as where the flux record initially reaches more than one half the maximum value and where the flux level drops below this value again. This method improves the ideal characterization because it is not prolonged by the residual burn off.

Large variations in TRS output affect the repeatability of the TRS maximum. Determination of the half maximum value changes between records. Because of the amount of this variation, crossover to below half maximum could occur more than once. This presents a problem in some algorithms for establishing the parameters but can be overcome. A draw-

back to this method is the exclusion of data outside the defined pulse length resulting in a low fluence calculation.

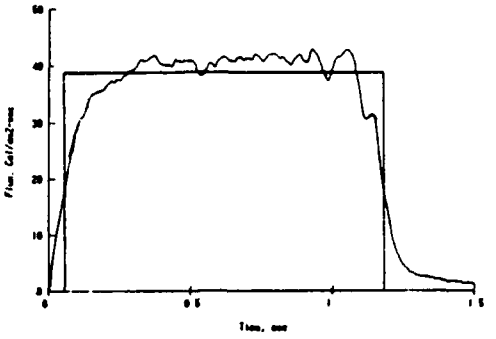

Figure 4. *Comparisons between TRS Data and Full Width Method at Half Maximum*

3.3 Moments Matching Method

The Moment Matching Method can establish the parameters of the rectangular pulse from an arbitrary pulse [2] in terms of its zeroth, first and second moments. The n'th moment is defined as

$$M_n = \int_{-\infty}^{+\infty} f_{(x)} t^n dt \tag{1}$$

ΩThe rectangle parameterized is the one which most closely matches the same moments. The amplitude A and the pulse width pw can be found centered about a point in time, t_c, from the following

$$t_c = \frac{M_1}{M_2} \tag{2}$$

$$pw = 2\sqrt{3(\frac{M_2}{M_3} - {t_c}^2)} \tag{3}$$

$$A = \frac{M_0}{pw} \tag{4}$$

The zeroth moment,M_0, is the fluence of the record, and establishing pw in somewhat rigorous fashion. The limitation of this characterization scheme is that pw is dependent on the second moment, M_2. The second moment is extremely sensitive to the range of data being observed. As the range of data points is increased, the instrumentation line noise will quickly affect the second moment value because of the t^2 term. The consequence is uncertainty regarding the calculated pulse width. The TRS data set must be carefully bounded to eliminate line noise outside what is considered pertinent data, before analysis can be performed.

3.4 Fourier Averaging Method

The Fourier Averaging Method is a completely formulated method of characterizing a TRS data set, requiring no estimation or handwork. The idea is much the same as the

Moments Matching method in that the data set is subjected to a process, then compared to a rectangular pulse subjected to the same process. The rectangular pulse that most closely matches that data defines the characterization parameters.

The Fourier transform of a time dependent equation into the frequency domain is defined as such

$$F_{(f)} = \int_{-\infty}^{+\infty} F_{(t)}{}^{-i2\pi ft} dt \tag{6}$$

When the integration is performed at $f = 0$, the result is the fluence. The method for finding the pulse width is done by finding the first point in the frequency domain where the magnitude of the transform is a minimum. This frequency point is equivalent to the reciprocal of the pulse width. For a true rectangular pulse [4]

$$pw = \frac{1}{f_0} \tag{7}$$

$$F_{(f_0)} = 0 \tag{8}$$

The Fourier transform of a TRS data set will yield approximately the same transform.

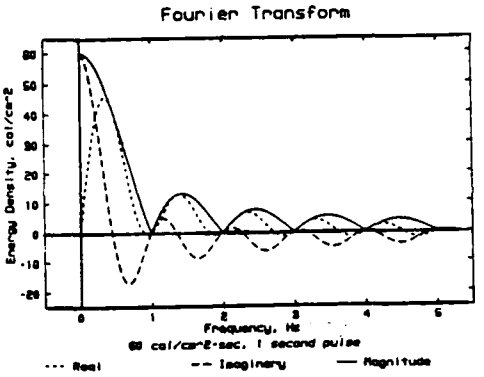

Figure 5. *Fourier Transform of a Rectangular Pulse*

By simply finding the first minimum point of the transformed record, the pulse width is established. The TRS data set is then fully characterized. The transform is relatively insensitive to the range of data used. Because of the insensitivity, data points can be bypassed to increase the speed of characterization.

The Fourier transform will break into two parts, real and imaginary. The magnitude is the root of the sum of the squares of the two parts. At zero hertz, the energy density will be at a maximum. This is also the fluence of the TRS record. As the frequency increases, the resulting integration will decrease until eventually a minimum is reached. Since the magnitude is the root of the sum of the squares, its value will never be negative. For a true rectangular pulse, this first minimum will be zero. Since TRS is a distortion of the rectangle, the minimum may not be zero, but the minimum is still clearly defined. The pulse width is defined as the reciprocal of the frequency where the magnitude of the transform is a minimum. For a more detailed treatment, see appendix A.

Finding the minimum is done by iteration, as shown in appendix C. Since the minimum is so clearly defined, few iterations are required. The process can be made more rapid by first

estimating the pulse width and concentrating the method in that area, but is not necessary. The result is a method of characterizing the TRS thermal pulse without any estimations or handwork. The technique is completely rigid, and the result repeatable with precision.

4. Simulation of a Target Response

To evaluate how accurate each method is in describing the TRS output, a computer generated thermal response simulation was performed. An imaginary aluminum plate was exposed to actual TRS data generated at BRL, and a temperature profile calculated. The four characterization methods were used to derive idealized thermal pulses. The aluminum plate was exposed to the thermal pulses. The resulting temperature profiles were compared with the original profiles.

The numerical method was shown to work, and to what degree of accuracy by comparing the numerical results to an analytical solution of the same problem. Once satisfied the numerical method worked, the comparisons of the temperature profiles where performed.

4.1 Analytical Solution

To evaluate the validity of the characterization schemes, a numerical simulation of the TRS data and the results of the four schemes are compared. To demonstrate the validity of the numerical method, an analytical solution of the same problem is solved. The results of the analytical solution can be compared to those of the numerical method. The simulation target is an infinite slab of aluminum with defined thickness. To simplify the calculations, the following assumptions are made;

All thermal radiant energy is absorbed.

Re-radiation from the slab is neglected.

All material properties are assumed constant regardless of temperature.

No other heat transfer processes, such as convection, are considered.

The slab is infinitely large, therefore limiting the calculation to one dimension (no edge effects).

The following is the transient heat conduction equation with the listed symbols indicated in Figure 6.

L = slab thickness
Θ = temperature
x = distance from adiabatic surface
t = time

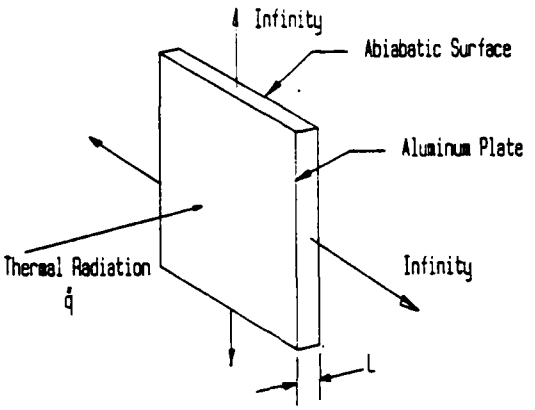

Figure 6. *Infinite slab considered for target response*

k = thermal conductance
C_p = specific heat
ρ = material density
$\dot{q}$ = radiant flux per unit area
α = thermal diffusivity, $\frac{k}{\rho C_p}$

The heat conduction equation is

$$\frac{\partial^2 \Theta}{\partial x^2} = \frac{1}{\alpha}\frac{\partial \Theta}{\partial t} \tag{9}$$

With the following boundary and initial conditions,

$1) t = 0, \Theta_{(x,t)} = 0$

$2) x = 0, \frac{\partial \Theta}{\partial x} = 0$

$3) x = L, \frac{\partial \Theta}{\partial x} = \frac{-\dot{q}}{k}$

the solution to the heat conduction equation is given by [5]

$$\Theta_{(x,t)} = \frac{\dot{q}L}{k}\left[\frac{\alpha t}{L^2} + \frac{3x^2 - L}{6L^2} - \frac{2}{\pi}\sum_{n=1}^{\infty}\frac{(-1)^n}{n^2}e^{-\alpha n^2 \pi^2 t/L^2}cos(\frac{n\pi x}{L})\right] \tag{10}$$

This represents the first part of the solution for target response, exposing the target to the thermal pulse. The second part of the solution is the target response after thermal exposure. This is done by solving the heat conduction equation for the slab with some arbitrary initial temperature distribution throughout the slab, $f(x)$. Given the following initial conditions and boundary conditions, and selecting a new time variable to take into account the offset of the post-pulse time,

$$w = t - pw \tag{11}$$

With the following boundary and initial conditions,

$1) w = 0, \Theta_{(x,w)} = f_{(x)}$

$f_{(x)}$ is the initial temperature distribution

in the slab, i. e. Equation 10 evaluated at $t = pw$

$2) x = 0, \frac{\partial \Theta}{\partial x} = 0$

$3) x = L, \frac{\partial \Theta}{\partial x} = -\frac{\bar{q}}{k}$

the solution to the heat conduction equation, again by [5], is

$$\Theta_{(x,w)} = \frac{1}{L}\int_0^L f_{(s)}ds + \frac{2}{L}\sum_{n=1}^{\infty} e^{-\alpha n^2 \pi^2 t/L^2} cos(\frac{n\pi x}{L}) \int_0^L f_{(s)} cos(\frac{n\pi x}{L}) ds \tag{12}$$

For a more detailed explanation about how this solution was determined, refer to appendix C. This analysis is good for the transient temperature distribution after the target is exposed to the TRS pulse. One more temperature that can be evaluated is the final uniform temperature distribution in the target well after the thermal pulse. The result can be easily derived as follows:

$$\Theta_{equilibrium} = \frac{\bar{q}\ pw}{\rho C_p L} \tag{13}$$

With the analytical solutions available, the numerical method can be validated.

4.2 Numerical Solution

The numerical solution is used to observe the effect of actual TRS data on the target. An explicit formulation of the difference equation is used to solve the transient temperature history given the same assumptions and boundary conditions as used in obtaining the analytical solution. The formulation is as follows;

$$T_i^+ = T_i + \alpha \frac{\Delta t}{\Delta x}\left[\frac{\bar{q}_i}{k} + \sum_j \frac{T_j - T_i}{\Delta x}\right] \tag{14}$$

T_i is the temperature of node i in the plate. T_i^+ is the explicit prediction of the temperature after some time increment Δt, and Δx is the incremental node thickness.

The TRS data was stored in an ASCII file. A BASIC program was written and run on a personal computer to perform the explicit calculation.

The simulation used in this report was a 15 centimeter thick aluminum slab. The same assumptions were applied as in the analytical solution. It was felt that this type of simulation would be most appropriate since target response of thermally thick targets is more affected by flux levels than thermally thin targets [7]. The condition for thermal thickness occurs when

$$\alpha \frac{t_{max}}{L^2} < 0.2 \tag{15}$$

where α is the thermal diffusivity, t_{max} is the time at which maximum irradiation from a nuclear event occurs, and L is the plate thickness. Thermally thin plates are affected mainly by the fluence of the source irradiator. If a plate is thermally thin, the temperature distribution is essentially uniform, and the problem is treated as a lumped capacitance. Targets exposed to different events with equal fluence will react equally. Thermally thick

Table 1. *Results of numerical and analytical comparisons*

		Peak Temp. Front			Temp of Slab		
A	pw	Num.	Anal.	δ	Num.	Anal.	δ
40	1	386.9	384.9	2.0	305.9	304.6	1.3
50	0.5	374.2	375.1	-0.9	303.5	302.9	-0.6
60	5	604.8	584.9	19.9	342.4	334.5	7.9
30	10	517.8	501.5	16.3	342.3	334.5	7.8
40	5	503.2	489.9	13.3	328.3	323.0	6.3
100	3	689.3	667.8	21.5	342.4	334.5	7.9
100	0.5	448.5	450.2	-1.7	307.1	305.8	1.3
50	1	408.6	406.2	2.4	307.2	305.8	1.4
25	2	378.6	375.1	3.5	307.1	305.8	1.3
20	5	401.6	395.0	6.6	314.2	311.5	2.7

targets respond differently to events with different flux levels, even though the fluence may be equal. These targets experience higher temperatures on the exposed surface for higher flux events. For equal fluence exposures, long after the thermal event, the target temperature will distribute to an equilibrium level.

The results of several different rectangular thermal pulses were used to check the numerical results against the analytical. The two methods yielded the same results consistently, indicating the numerical method worked reasonably well. A computer simulation of the described target was exposed to ten random thermal pulses. The resulting temperature profiles yielded a peak temperature and a uniform temperature after a long time. These two temperatures are compared in Table 1. The small δ is the difference between the numerical and analytical results.

Comparisons are poor for long duration burns due to error growth of the finite difference. The TRS data used in this analysis are all short duration, within two seconds. From Table 1, equivalent comparisons are quite close, within 1%. The magnitude of the flux level also amplifies the numerical error, but the data used in the evaluation are well below fifty calories, again maintaining a good affin' y between the methods.

4.3 Target and Thermal Radiation Simulator Data

The target used in this simulation is an aluminum slab with the following material properties.

L = thickness, 15 centimeters

ρ = density, 2,707 $\frac{kg}{m^3}$

C_p = specific heat, 0.896 $\frac{kJ}{kg-K}$

k = thermal conductance, 204 $\frac{W}{m-^oC}$

α = thermal diffusivity, 8.418x10-5 $\frac{m^2}{s}$

The assumptions are the same as for the analytical solution.

All thermal radiant energy is absorbed.

Re-radiation from the slab is neglected.

All material properties are assumed constant regardless of temperature.

No other heat transfer processes, such as convection, are considered.

The slab is infinitely large, therefore limiting the calculation to one dimension (no edge effects).

The TRS data was obtained from the U.S. Army Ballistic Research Laboratorys aluminum/liquid oxygen Thermal Radiation Simulator. Five such records are presented ranging from good rectangular pulses to poor representations. This is to show the extremes that can be found in real life, and compare the results of the four characterization schemes. Figure 7 shows the five TRS record traces. The five data records represent the thermal output sensed by a Medtherm Calorimeter placed 100 cm. from the nozzle center and 29 cm. above the nozzle top, as depicted in Figure 8. This is the reference station used in evaluating and comparing the TRS records at BRL. The incongruity in output is caused by certain changes experimented with in an effort to improve the consistency and efficiency of TRS burns.

Trace 1 and 3 are the worst case data sets. Both are considered poor in quality, but are presented here to show the difficulties in achieving consistent parametric levels. Trace 2 is an anomalous TRS burn with large variants, and Traces 4 and 5 are considered close approximations of a rectangular pulse.

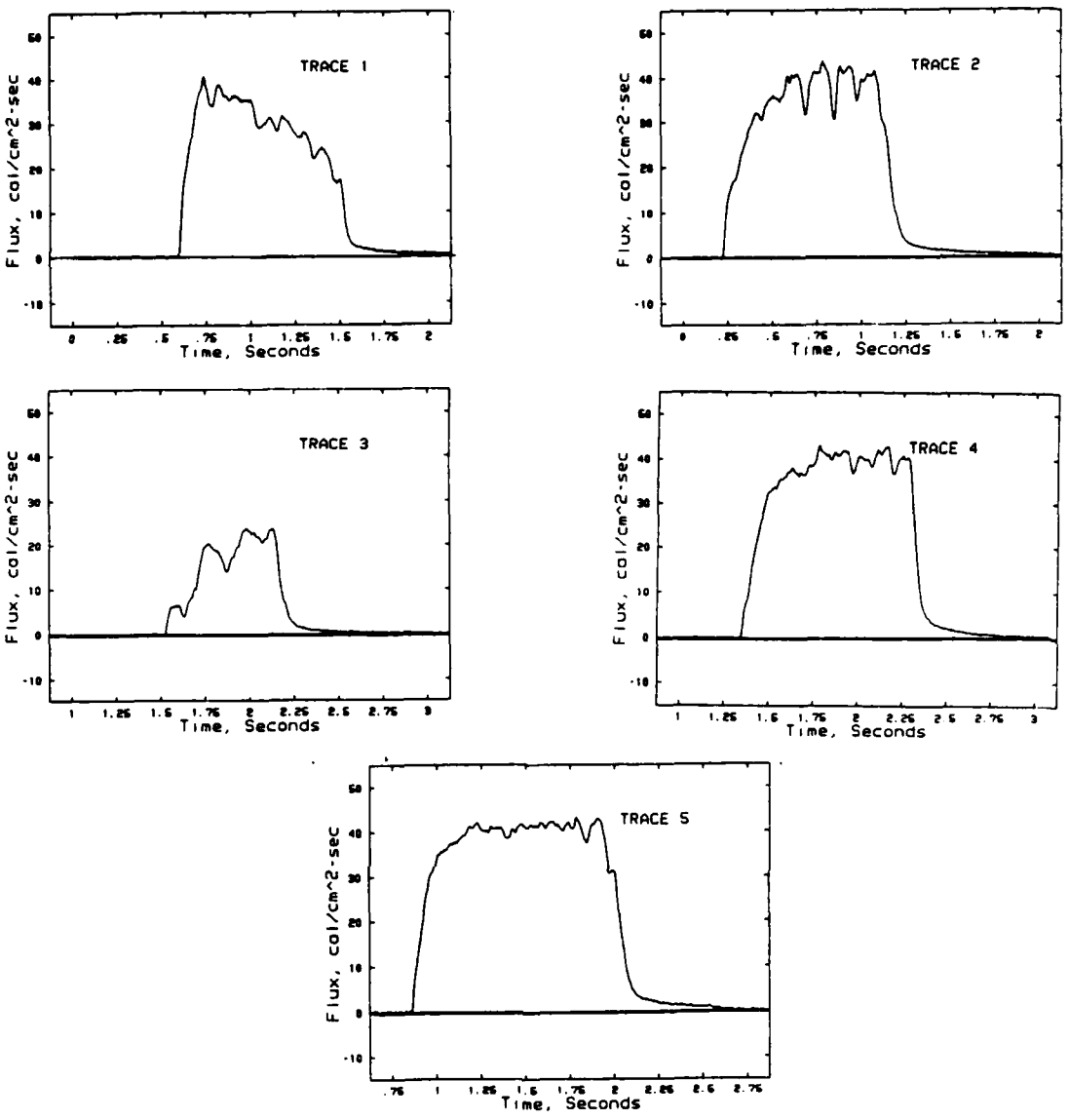

Figure 7. *Five U.S. BRL TRS Record Traces used for Characterization scheme comparisons.*

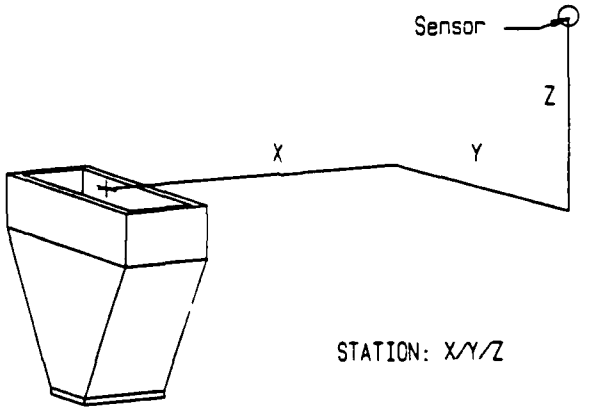

Figure 8. *Spatial location method used in locating calorimeter position relative to BRL TRS Nozzle.*

5. Results of the Parameterization of the Five TRS Data Traces

A Fortran program was written to evaluate the characteristic parameters concurrently. All four methods were evaluated using the same data range to maintain equal fluence, except in the Full Width Half Maximum method, by definition. The results of establishing the TRS data parameters is listed in Table 2. The parameters listed below were used to generate

Table 2. *TRS Data Parameters as established by the Characterization Schemes.*

	Full Width		Half Max.		Mom. Match.		Fourier Ave.	
	Flux	Time	Flux	Time	Flux	Time	Flux	Time
Trace 1	28.01	0.965	31.02	0.810	31.39	0.861	32.03	0.844
Trace 2	25.90	1.275	36.38	0.835	36.47	0.905	38.90	0.849
Trace 3	15.23	0.700	19.75	0.465	18.50	0.576	19.87	0.537
Trace 4	32.96	1.800	38.05	0.89	38.82	0.917	39.80	0.895
Trace 5	34.61	1.285	38.85	1.100	39.93	1.114	40.67	1.094

twenty ideal simulation rectangular thermal pulses, and by the same method as before, used to derive by explicit numerical calculation, the temperature profile of the aluminum target. These profiles were then compared to the simulation that used real TRS data. Figures 9, 10 and 11 shows the comparisons. The results of the comparisons show the difference between the ideal pulse and the TRS pulse is small, except for the Full Width method. The consistent "best fits" are the Moments Matching and Fourier Average methods. The Full Width method consistently underestimates the flux level, resulting in a lower surface temperature. The Full Width at Half Maximum consistently under calculates the fluence, resulting again in lower surface temperature rise as well as a lower final temperature distribution.

The advantage of the Moments Matching is the calculation for the parameters is relatively straight forward. Only three integrations are necessary, and the parameters are computed from the resulting moments. The problem is that by changing the range of data, or the data set size, used in the computation, the parameters change. The second moment is extremely sensitive to line noise, so care must be taken to filter the data.

The Fourier Average method is insensitive to noise. Figure 12 shows the effect of using the entire data record for Trace 4 compared to the carefully ranged data set. The Full Width method result in a pulse length of the entire record of low average flux. The results is a different temperature profile as shown below. The Moments Matching experiences a pulse lengthening since, by Equation 3 pulse length is computed using the second moment, as well as a slight increase in the fluence. The Fourier Average shows only a slight increase in the flux level due to summing the noise into the fluence, but the pulse length essentially remains the same. In effect the Fourier Average method establishes the same pulse width, despite the increase in data record. The drawback to using the Fourier Average method is that the computation involves an iterative process using integrations. This will result in longer computations on the computer. Depending on the size of the data set, that time may be insignificant.

Since the Fourier Average method is insensitive to high frequency fluctuations, one could select a fraction of the data (pick one out of every ten sample points) to reduce the computation time for pulse length. Figure 13 shows the comparison of the Fourier transform of Trace 2 and Trace 3. The original sample rate was 200 points per second. Data decimation of ten to one reduces the data sample rate to 20 points per second. Trace 3 showed a wider variation in the derivative of the Fourier transform of the magnitude, but the end result was an extremely close match for average flux and pulse width. One must add that the same decimated data yield equally close results when used with the other characterization schemes, as demonstrated below in Table 3.

Table 3. *Comparisons of Characterization Schemes results between full data set and decimated data set.*

		Flux (cal/cm^2sec)		Pulse (sec)	
		Full	Decimated	Full	Decimated
Full Width	Trace 2	25.9	25.43	1.28	1.3
	Trace 3	15.23	14.33	0.7	0.75
Half Maximum	Trace 2	36.38	36.85	0.835	0.925
	Trace 3	19.75	19.65	0.47	0.5
Moments Matching	Trace 2	36.47	35.98	0.90	0.919
	Trace 3	18.5	18.32	0.576	0.587
Fourier Average	Trace 2	38.9	38.38	0.849	0.861
	Trace 3	19.87	19.73	0.537	0.545

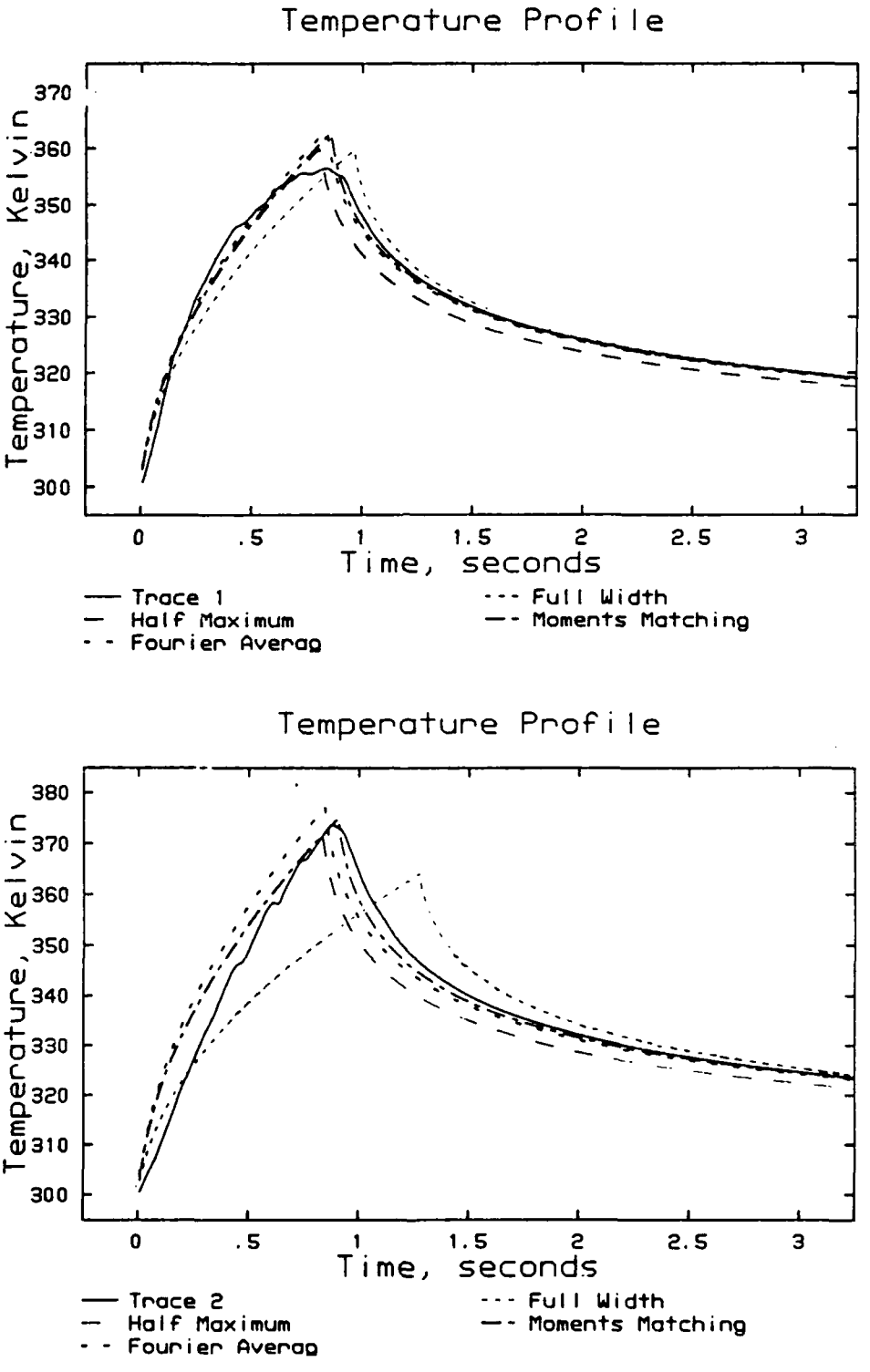

Figure 9. *Comparisons of the results of numerically computed temperature profiles on the target surface using Trace 1 and Trace 2 with their respective idealized thermal pulses.*

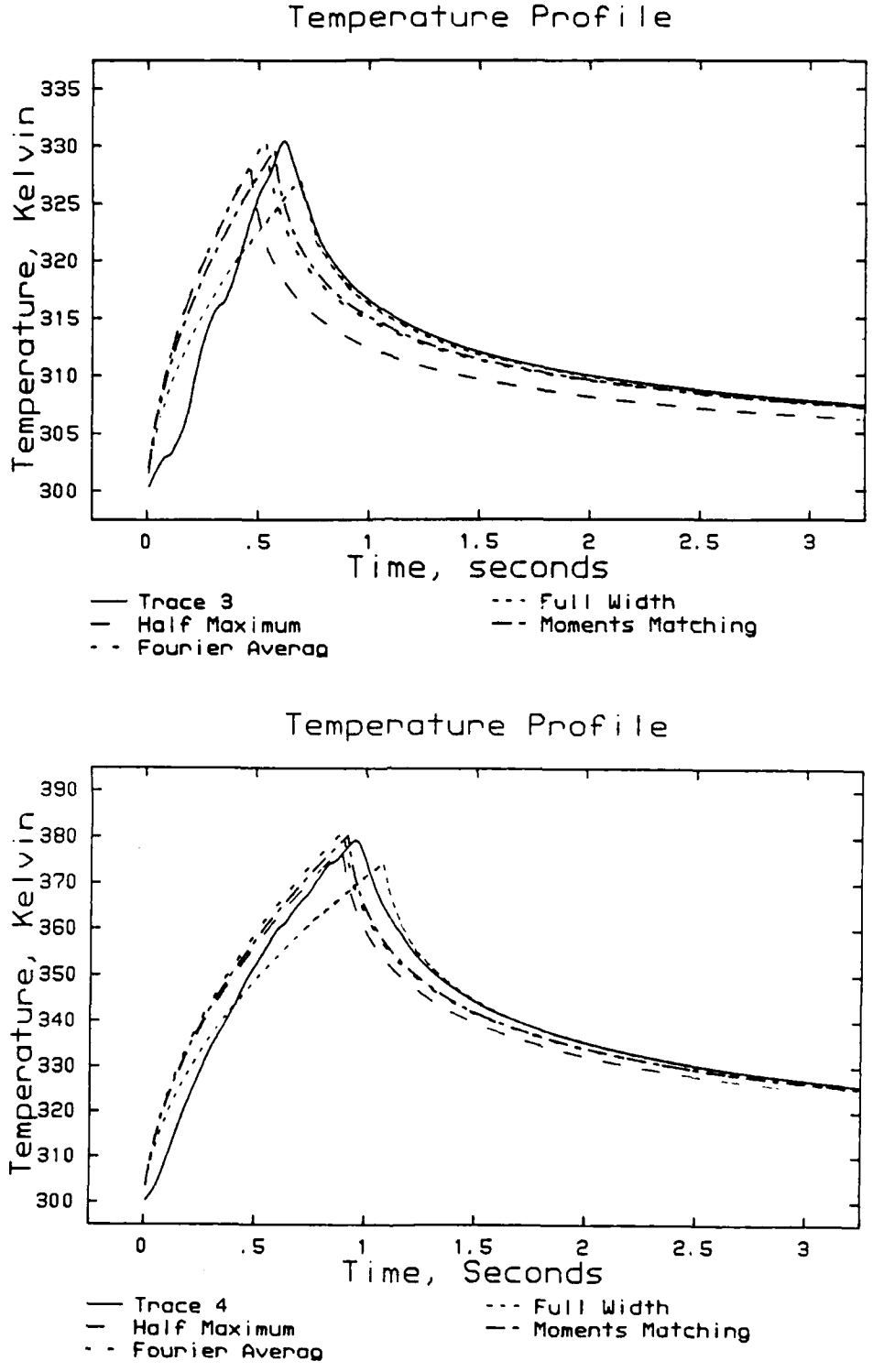

Figure 10. *Comparisons of the results of numerically computed temperature profiles on the target surface using Trace 3 and Trace 4 with their respective idealized thermal pulses.*

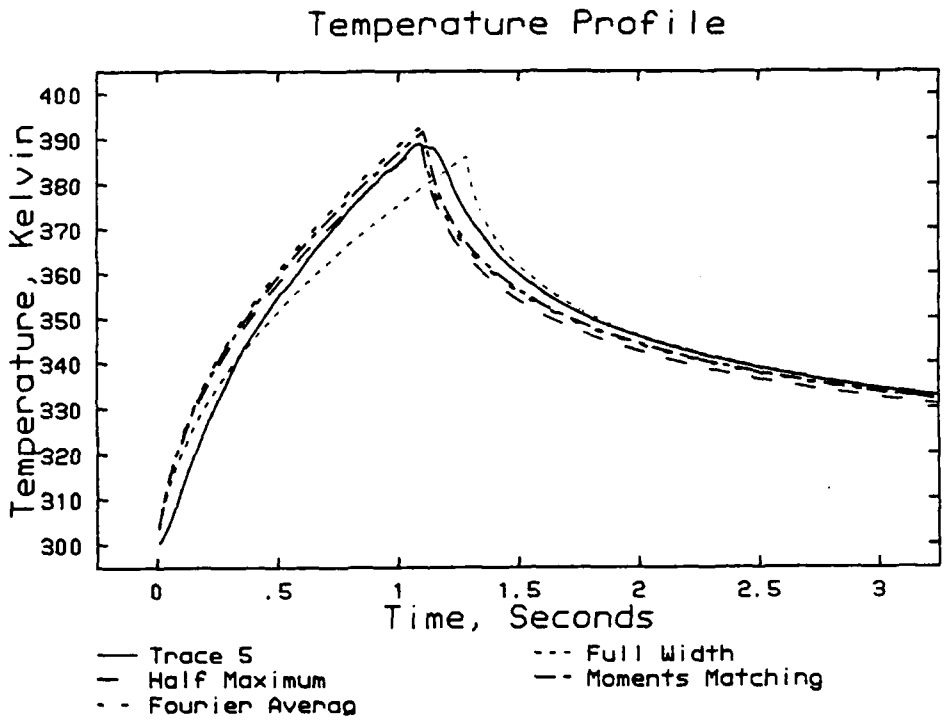

Figure 11. *Comparisons of the results of numerically computed temperature profiles on the target surface using Trace 5 with its respective idealized thermal pulses.*

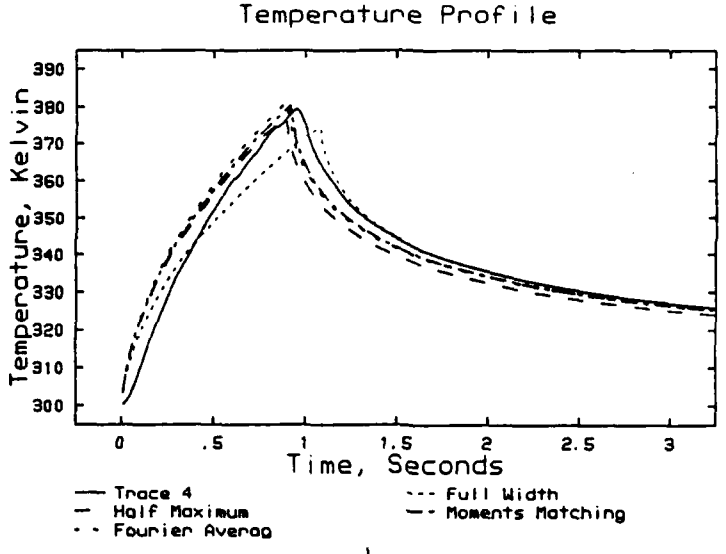

a)

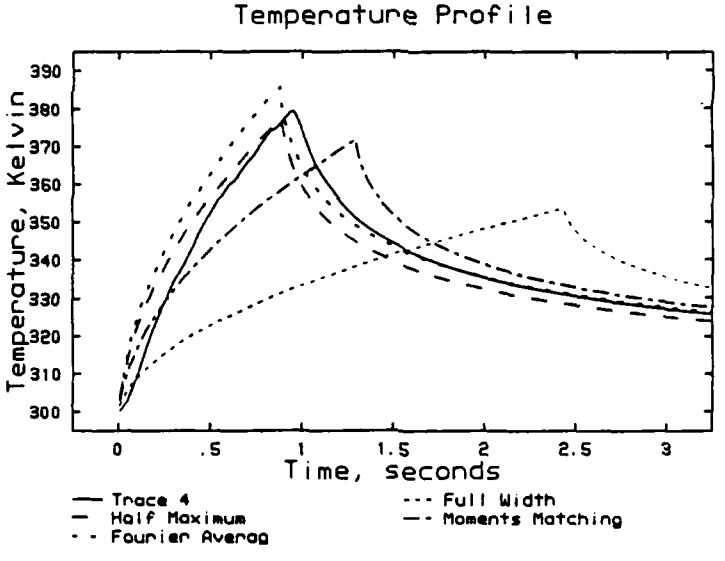

b)

Figure 12. *Comparisons of the results of numerically computed temperature profiles on the target surface using Trace 4 and the respective four idealized thermal pulse taken over a) a selected range of data and b) the entire range of data.*

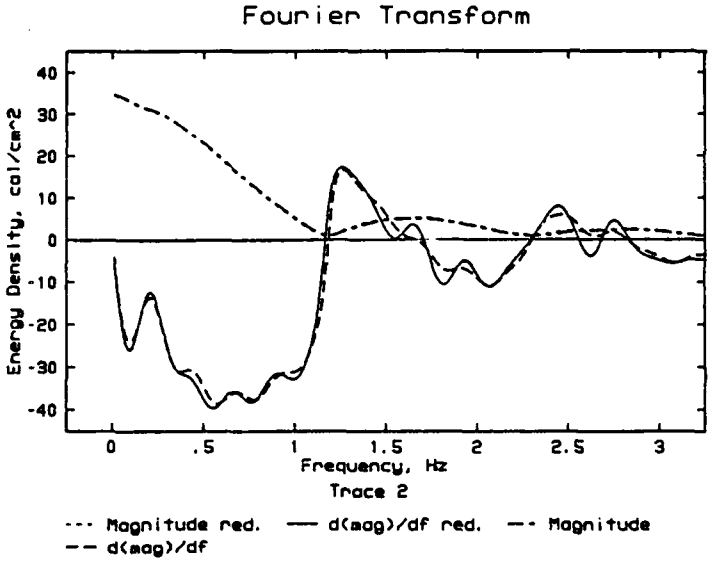

a)

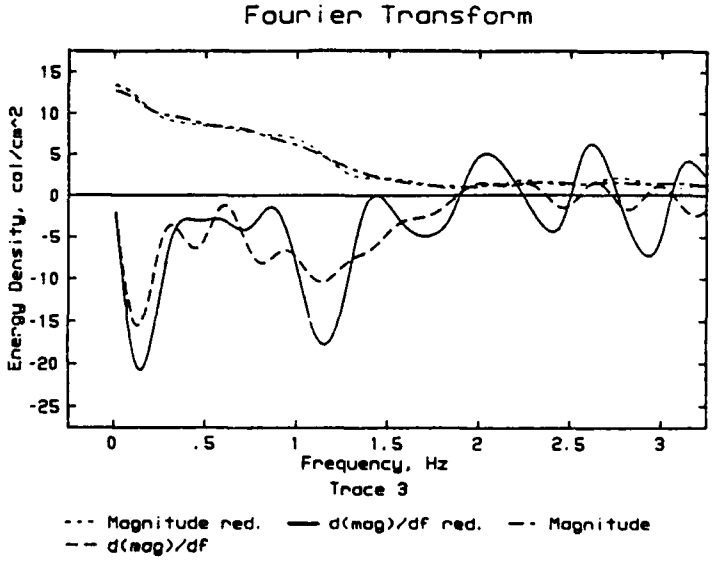

b)

Figure 13. *Comparisons of the Fourier Transform of a) Trace 2 and decimated Trace 2, b) Trace 3 and decimated Trace 3.*

6. Conclusions

After evaluating the four parameterization schemes against a computer thermal response target simulation, the Fourier Average technique emerges as the most consistent method. Regardless the size of the data set and noise, the parameters of the TRS data are calculated with greater consistency than with any other method. Decimating the data had little effect on the output. The simulated target temperature profiles of the calculated ideal thermal flux records showed the Fourier parameterized pulse was consistent with the actual TRS data simulation.

With the increase of data, the pulse width of the Fourier Average calculated ideal pulse showed a slight increase in average flux level. The Moments Matching methods showed a large deviation of pulse length from the original, carefully isolated data set. This is because the second moment is particularly sensitive to instrumentation line noise. An inflated value for the second moment will result in an increase of the pulse length. The Other methods remained the same by definition. The Full Width and Full Width at Half Maximum methods ignores all data outside the selected data range. The slight increase in average flux was due to the line noise is also being integrated. The effect is reflected in the Moments Matching method as well.

The drawback of the Fourier Average technique is the iterative method used to find the pulse width. With an extremely large data set, this could result in long computation time. Elimination of ninety percent of the data set did not affect the method results by more than 1 %. This would increase the speed of computation with little to no effect on the outcome. A typical Thermal Radiation Simulator data set consists of about 200 points per second. For a three second data set, the calculation time difference on a personal computer is indiscernible.

The result of the Fourier Average generated ideal thermal pulse against the actual TRS data in the aluminum plate simulation showed good consistency. The Fourier Average method was not consistently better at parameterizing an ideal match. For different TRS data sets, some other methods worked better. This is due to uniqueness in a data set. The resulting temperature profiles showed moderate fits by all methods except the Full Width method.

The strength in the Fourier Average method is in its consistency despite range of data, or data elimination, and the complete rigor in which the parameters are calculated.

INTENTIONALLY LEFT BLANK.

References

1. B. Schallhorn, A. Baba, S. Share, *Correlation of Thermal Response Data at Various DoD Thermal Radiation Test Facilities*, U.S. Army Laboratory Command, Harry Diamond Laboratories, Adelphi, MD, December, 1989, HDL-TR-2160

2. K.Matthews, G. Brumburgh, *A Data Analysis Method for Evaluation of TRS Calorimeter Data*, Field Command, Defense Nuclear Agency, Test Technical Directors Division, Kirtland AFB, NM, 1989

3. W. Rehmann, *Characterization of the Thermal Radiation Field Generated by a One-Nozzle Torch*, U.S. Army Ballistic Research Laboratory, Aberdeen Proving Ground, MD, October, 1983,ARBRL-TR- 02529

4. E.O. Brigham, *The Fast Fourier Transform*, Prentice-Hall, Inc., Englewood Cliffs, New Jersey,1974

5. H.S. Carslaw, J.C. Jaeger, *Conduction of Heat in Solids*, 1947, Oxford University Press, London, England

6. A.J. Chapman, *Heat Transfer*, Fourth Edition, 1974, Macmillan Publishing Company, 866 Third Avenue, New York, New York 10022

7. A.J. Baba, S. Share, *Nuclear Thermal Design/Validation Guidelines for Army Tactical Applications*, U.S. Army Laboratory Command, Harry Diamond Laboratory, Adelphi, Maryland, July, 1986, HDL-TR-20931

INTENTIONALLY LEFT BLANK.

APPENDIX A

Appendix A

Fourier Transform of a Rectangular pulse and Comparison with TRS data

The Fourier transform of a time dependent equation into the frequency domain is defined as such

$$F_{(f)} = \int_{-\infty}^{+\infty} F_{(t)}{}^{-i2\pi ft} dt \qquad (A-1)$$

Given a discontinuous function described as

$F_{(t)} = 0, t \leq t_i$

$F_{(t)} = A, t_i < t < t_f$

$F_{(t)} = 0, t \leq t_f$

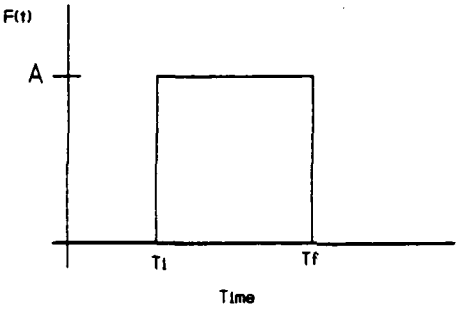

then integration yields;

$$F_{(f)} = \frac{iA}{2\pi f}(e^{-i2\pi ft_f} - e^{-i2\pi ft_i}) \qquad (A-2)$$

were $i = \sqrt{-1}$ The transform evaluated at $f = 0$ is such;

$$\lim_{f \to 0} F_{(f)} = 2\pi A(1-1)/0 \qquad (A-3)$$

which is undefined. Let

$$g_{(f)} = i2\pi A(e^{-12\pi ft_i} - e^{-i2\pi ft_f}) \qquad (A-4)$$

$$h_{(f)} = 2\pi f \qquad (A-5)$$

Then differentiation with respect to f yields;

$$g'_{(f)} = 2\pi A(-t_i e^{-i2\pi ft_i} + t_f e^{-i2\pi ft_f}) \qquad (A-6)$$

$$h'_{(f)} = 2\pi \qquad (A-7)$$

Using L'Hospital's rule for undefined limits,

$$\lim_{f \to 0} \frac{g'_{(f)}}{h'_{(f)}} = A(t_f - t_i) \qquad (A-8)$$

Therefore,

$$F_{(0)} = Apw \qquad (A-9)$$

and can also be thought of as the area under the curve of the defined function. Using Euler transformation,

$$F_{(f)} = \frac{A}{2\pi f}\Big[sin(2\pi ft_i) - sin(2\pi ft_f) + i[cos(2\pi ft_i) - cos(2\pi ft_f)]\Big] \qquad (\ - 10)$$

and defining f_0 such that

$$F_{(f_0)} = 0 \qquad (A-11)$$

This can only happen when the real and the imaginary parts are zero. The magnitude of $F_{(f)}$ is defined as;

$$\|F\| = \frac{A}{2\pi f}\sqrt{real^2 + imaginary^2}$$

$$\|F\| = \frac{A}{2\pi f}\sqrt{2 - 2cos[2\pi f(t_i - t_f)]} \qquad (A-12)$$

and at $f = f_0$,

$$\|F\| = 0$$

only if

$$2\pi f_o(t_f - t_i) = 2\pi n \qquad n = 1, 2, 3, ... \qquad (A-13)$$

if $t_f - t_i$ is the pulse width, pw, then by A-13,

$$pw = \frac{1}{f_0} \qquad (A-15)$$

Thus for the Fourier Averaging technique, one must evaluate the fourier transform with $f = 0$, which yields the fluence of the Thermal Radiation Simulator data. Then one must find the minimum value of the magnitude of the transform and determine what the value for f_0 is. This yields the pulse length, which leads to the average flux.

One could take this type of analysis farther and attempt to evaluate the starting point of the TRS record, but that meaning is useless in this aspect. One need only find the frequency in which the real or the imaginary part of the transform is zero, then compare the result to a rectangular pulse starting at $t = 0$. The solution is quickly derived, but withheld in this presentation.

INTENTIONALLY LEFT BLANK.

APPENDIX B

Appendix B

Algorithm Method for finding Pulse Width, Fourier Averaging

Finding the pulse width is the key to the successful characterization of the thermal pulse. In the method of Fourier Averaging, the pulse width is determined by finding the first minimum of the magnitude of the fourier transform. Since the TRS data is not a perfect rectangular pulse as supposed in appendix A, the minimum may not be zero. So the algorithm used must search for a minimum value as opposed to a zero value increasing the difficulty of the task. Many root searching algorithms determine a zero point if the values searched are within a minimum tolerance. The assumption is that the values eventually pass through zero, and the value found in the tolerance is sufficient. Unfortunately, the TRS data transform minimum may be greater than the tolerance, and the algorithm would pass by in search of a better match.

The problem is solved by knowing the area where the magnitude minimum is located also represents a drastic change in the values of the magnitudes derivative with respect to the frequency. The derivative of A-12,

$$\frac{\partial \|F\|}{\partial f} = \frac{A}{2\pi f}\sqrt{2 - 2cos[2\pi f(t_f - t_i)]}\left[\frac{(t_f - t_i)sin[2\pi f(t_f - t_i)]}{cos[2\pi f(t_f - t_i)]}\right] \qquad (B-1)$$

shows a discontinuity at $f = 1/(t_f - t_i) = f_0$, A-15 as shown in Figure 14. The TRS data transforms may not be discontinuous, but the point where the change in signs occurs can be found. Initially, the point f_0^1 is guessed at by approximating the pulse width as that of

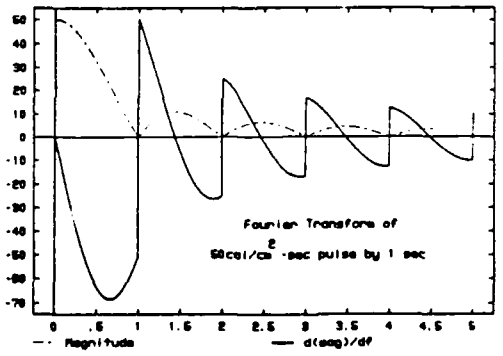

Figure 14. *Magnitude and Derivative of Fourier Transform of 50 cal/cm2 – sec by 1 sec pulse.*

the Full Width method. Then a second point, f_0^2 is picked nearby, within a small δf. The respective $\|F\|$ are found. The results are used to determine the approximate derivative at f_0^1 by;

$$\frac{\partial \|F_1\|}{\partial f} \approx \frac{\|F_2\| - \|F_1\|}{f_0^2 - f_0^1} \qquad (B-2)$$

A third point, f_0^3 is initially found by using the reciprocal of the pulse width determined by the Full Width at Half Maximum data. a fourth point, f_0^4 is found near f_0^3 by a small δf. The magnitudes are evaluated, and the approximate derivative of f_0^3 is found. Then the

results of the two derivatives are used to interpolate for f_0^5. A point f_0^6 near f_0^5 is picked, within some δf, and the magnitudes and approximate derivative of f_0^5 are determined. If the derivative of f_0^5 is not within the specified tolerance, the process is repeated with f_0^5 being replaced by the closest of f_0^1 or f_0^3.

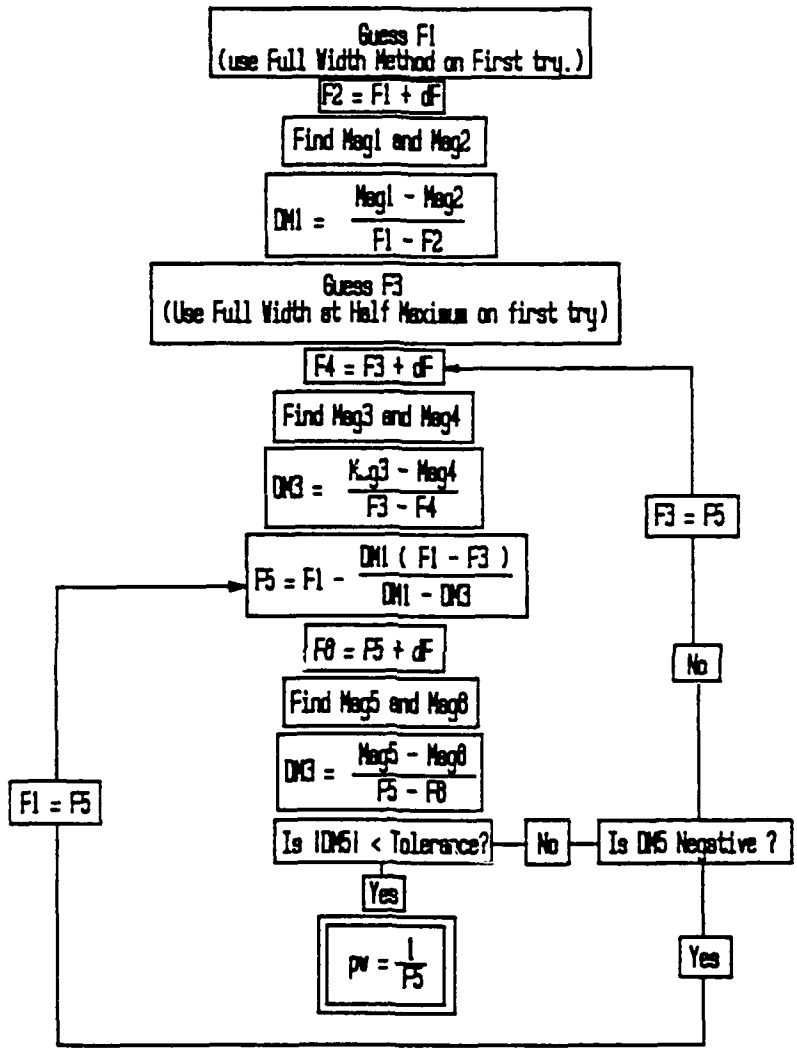

Figure 15. *Flow Chart for determining Pulse Width*

INTENTIONALLY LEFT BLANK.

APPENDIX C

Appendix C

Solution of the Heat Conduction Equation given an Initial Temperature Distribution.

For the 1 dimensional heat conduction equation

$$\frac{\partial^2\Theta}{\partial x^2} = \frac{1}{\alpha}\frac{\partial\Theta}{\partial t} \qquad (C-1)$$

with the following boundary conditions,

$$x = 0,\ \frac{\partial\Theta}{\partial x} = 0 \qquad (C-2)$$

$$x = L,\ \frac{\partial\Theta}{\partial x} = 0 \qquad (C-3)$$

and initial condition,

$$t = 0,\ \Theta = f_{(x)} \qquad (C-4)$$

a solution for C-1 is,

$$\Theta = e^{-\alpha 2t}(A_1 sin(\lambda x) + A_2 cos(\lambda x)) \qquad (C-5)$$

$$\frac{\partial\Theta}{\partial x} = e^{-\alpha 2t}(A_1 cos(\lambda x) + A_2 sin(\lambda x)) \qquad (C-6)$$

substituting boundary condition C-2 sets $A_1 = 0$.

Boundary condition C-3 sets $A_2 sin(\lambda L) = 0$. $A_2 = 0$ leads to the trivial solution. For the nontrivial solution, $sin(\lambda L) = 0$, only if

$$\lambda_n = \frac{n\pi}{L}, \qquad n = 1, 2, 3, ... \qquad (C-7)$$

Thus the solution by boundary conditions is

$$\Theta = \sum_{n=1}^{\infty} e^{-\alpha n^2\pi^2 t/L^2} A_n cos\left(\frac{n\pi x}{L}\right) \qquad (C-8)$$

the initial condition, C-4, will determine the solution of A_n. In short, A_n is determined by use of the orthogonality relationship for a cosine function [6]. A countably infinite set of functions is considered orthogonal in the interval $a < x < b$ if

$$\int_b^a g_m(x) g_n(x) dx = 0 \ when \ \ m = n \qquad (C-9)$$

let $f_{(x)}$ be some arbitrary function within this interval. $f_{(x)}$ can be expressed in terms of

$$f_{(x)} = C_1 g_1(x) + C_2 g_2(x) + ... + C_n g_n(x) + ... + C_m g_m(x) + ... = \sum_{j=1}^{\infty} C_n g_n(x) \qquad (C-10)$$

The C's are constants to be determined. If the series C-10 is convergent, and integrable after multiplication with one of the functions, $g_k(x)$, then by definition of C-9,

$$\int_a^b f_{(x)} g_k(x) dx = C_k \int_a^b g_k^2(x) dx \qquad (C-11)$$

and the constant, C_k can be found by the following,

$$C_k = \frac{\int_a^b f(x) g_k(x) dx}{\int_a^b g_k^2(x) dx} \qquad (C-12)$$

One can show that the set of functions,

$$\{cos\lambda nx\},\ \lambda_n = \frac{n\pi}{L},\quad n = 0, 1, 2, 3, ... \qquad (C-13)$$

is an orthogonal set over $0 < x < L$. Also the arbitrary function can be represented by cosines as

$$f_{(x)} = \sum_{n=1}^{\infty} C_n cos(\lambda_n x) \qquad (C-14)$$

with

$$C_0 = \frac{1}{L}\int_0^L f_{(x)} dx$$

$$C_n = \frac{2}{L}\int_0^L f_{(x)} sin(\lambda_n x) dx \qquad (C-15)$$

With the above, the specific results for the target response after the thermal loading can be determined. The temperature distribution, $f_{(x)}$ can be found from the previously derived solution of the heat conduction with constant flux on one surface. the uniform distribution is

$$f_{(x)} = \frac{\ddot{q}L}{k}\Big[\frac{\alpha t}{L^2} + \frac{3x^2 - L}{6L^2} - \frac{2}{\pi}\sum_{n=1}^{\infty}\frac{(-1)^n}{n^2} e^{-\alpha n^2 \pi^2 pw/L^2} cos(\frac{n\pi x}{L})\Big] \qquad (C-16)$$

This can be substituted into C-14, and integrated in different parts. The results are substituted into C-8 resulting in;

$$\Theta_{(x,w)} = \frac{1}{L}\int_0^L f_{(s)} ds + \frac{2}{L}\sum_{n=1}^{\infty} e^{-\alpha n^2 \pi^2 t/L^2} cos(\frac{n\pi x}{L}) \int_0^L f_{(s)} cos(\frac{n\pi x}{L}) ds \qquad (C-17)$$

Thus the solution for heat conduction in the slab after exposure to the thermal load, where w is the displaced time, $w = t - pw$.

INTENTIONALLY LEFT BLANK.

APPENDIX D

Appendix D

BASIC and Fortran IV Programs

PARAM.FOR: This Fortran program was the instrument used to evaluate the four characterization methods. Note that the data are all based on a sampling rate of 200 Hertz, and no record is over five seconds long.

```
      CHARACTER TRACE*15
      CHARACTER METH*20
      COMMON / FLUX / F(4000),A(3)
      PRINT *,' Input the TRS record to be Characterized:'
      READ *,TRACE
      OPEN(UNIT=30,ERR=300,FILE=TRACE,STATUS='OLD')
      L1=0
      FMAX=0
      NSTRT=0
      NEND=0
      N=0
5     N=N+1
      READ(30,100,ERR=11,END=12) F(N)
100   FORMAT(F12.5)
      IF(F(N).GT.3.0) THEN
      L1=1
      GO TO 10
      ELSE
      IF(L1.EQ.1) GO TO 10
      NSTRT=N
      END IF
10    IF(F(N).LE.FMAX) GO TO 20
      FMAX=F(N)
      NMAX=N
20    IF(F(N).GT.3.0) GO TO 5
      IF(N.LT.300) GO TO 5
      IF(NEND.NE.0) GO TO 5
      NEND=N
      GO TO 5
12    NSTP=N
      L2=0
      DO 200 N=NSTRT,NEND
      IF(F(N).GT.FMAX*0.5) THEN
      L2=1
      NHME=N
      ELSE
      IF(L2.EQ.1) GO TO 200
      NHMS=N
      END IF
```

```
200  CONTINUE
     SR=200
C    FULL WIDTH METHOD
     NDN=NEND-NSTRT
     DN=REAL(NDN)
     SUM=0
     DO 220 N=NSTRT,NEND
     SUM=SUM+F(N)
220  CONTINUE
     PWFW=DN/SR
     FLUE1=SUM/SR
     AFFW=FLUE1/PWFW
C    FULL WIDTH AT HALF MAXIMUM
     NDN=NHME-NHMS
     DN=REAL(NDN)
     SUM=0
     DO 320 N=NHMS,NHME
     SUM=SUM+F(N)
320  CONTINUE
     FLUE2=SUM/SR
     PWFWHM=DN/SR
     AFFWHM=FLUE2/PWFWHM
C    MOMENTS MATCHING METHOD
     DO 410 I=0,2
     SUM=0
     DO 420 N=NSTRT,NEND
     T=REAL((N-NSTRT)/SR)
     SUM=SUM+F(N)*T**I
420  CONTINUE
     A(I)=SUM/SR
410  CONTINUE
     TC=A(1)/A(0)
     PWMMM=2*SQRT(3*(A(2)/A(0)-TC**2))
     FLUE3=A(0)
     AFMMM=FLUE3/PWMMM
C    FOURIER AVERAGING
     PI=3.1415927
     DF=0.001
     F5=1/PWFW
450  F1=F5
     F2=F1+DF
     CALL SIMP(F1,NSTRT,NEND,AG1)
     CALL SIMP(F2,NSTRT,NEND,AG2)
     DM1=(AG1-AG2)/(F1-F2)
     F3=1/PWFWHM
455  F4=F3+DF
```

```
      CALL SIMP(F3,NSTRT,NEND,AG3)
      CALL SIMP(F4,NSTRT,NEND,AG4)
      DM3=(AG3-AG4)/(F3-F4)
460   F5=F1-DM1*(F1-F3)/(DM1-DM3)
      F6=F5+DF
      CALL SIMP(F5,NSTRT,NEND,AG5)
      CALL SIMP(F6,NSTRT,NEND,AG6)
      DM5=(AG5-AG6)/(F5-F6)
      IF(DM5.LT.-0.1) THEN
      F1=F5
      F2=F1+DF
      CALL SIMP(F1,NSTRT,NEND,AG1)
      CALL SIMP(F2,NSTRT,NEND,AG2)
      DM1=(AG1-AG2)/(F1-F2)
      GO TO 460
      ELSE
      IF(ABS(DM5).LT.0.05) GO TO 470
      F3=F5
      GO TO 455
      END IF
470   PWFA=1/F5
      CALL SIMP(0,NSTRT,NEND,FLUE4)
      AFFA=FLUE4/PWFA
      PRINT *,'METHOD              FLUENCE    PULSE WIDTH  AVERAGE FLUX '
      METH='FULL WIDTH'
      WRITE(*,500) METH,FLUE1,PWFW,AFFW
      METH='FULL WIDTH HALF MAX'
      WRITE(*,500) METH,FLUE2,PWFWHM,AFFWHM
      METH='MOMENTS MATCHING'
      WRITE(*,500) METH,FLUE3,PWMMM,AFMMM
      METH='FOURIER AVARAGING'
      WRITE(*,500) METH,FLUE4,PWFA,AFFA
500   FORMAT(1X,A20,1X,F12.6,1X,F12.6,1X,F12.6)
      STOP
300   PRINT *,'ERROR IN THE OPEN STATEMENT INPUT FILE'
      STOP
11    PRINT *,'ERROR READING FILE'
      STOP
      END

      SUBROUTINE SIMP(FR,NSTRT,NEND,AG)
      COMMON / FLUX / F(4000),M(3)
      PI=3.1415927
      SR=200
      THETA=FR*2*PI/SR
      SUMR=0
```

```
      SUMI=0
      DO 600 N=NSTRT,NEND
      D=REAL(NSTRT-N+1)
      SUMR=SUMR+F(N)*COS(THETA*D)
      SUMI=SUMI+F(N)*SIN(THETA*D)
600   CONTINUE
      RE=SUMR/SR
      RI=SUMI/SR
      AG=SQRT(RE**2+RI**2)
      RETURN
      END
```

An example of the output is shown below. The Data input was Trace 3.

Input the TRS record to be Characterized:

TRACE3

METHOD	FLUENCE	PULSE WIDTH	AVERAGE FLUX
FULL WIDTH	10.659768	0.700000	15.22824
FULL WIDTH HALF MAX	9.182742	0.465000	19.747833
MOMENTS MATCHING	10.659768	0.576070	18.504309
FOURIER AVARAGING	10.659768	0.536578	19.866194

MULTIPLT.BAS: This BASIC program was used to generate the temperature profiles using series of artificially generated thermal record. The output was read to an ASCII file called "OUT?" and plotted.

```
10 CLS
20 DIM T(100)
30 KEY OFF
40 FOR J = 13 TO 24
50 F$="A:PULSE"
60 G$="D:OUT"
70 IF INT(J/10)=1 THEN F$="A:PULSE1"
80 IF INT(J/10)=1 THEN G$="D:OUT1"
90 IF INT(J/10)=2 THEN F$="A:PULSE2"
100 IF INT(J/10)=2 THEN G$="D:OUT2"
110 J$=STR$(J)
120 J$=RIGHT$(J$,1)
130 FILE$=F$+J$
140 FILE2$=G$+J$
150 DUR=5
160 SR=200
170 INC = 1
180 N = SR * DUR
190 R = 1
200 REM ********** initialize the temperature profile **********
```

```
210 FOR K = 1 TO 100
220 T(K) = 300
230 NEXT K
240 REM ********** set constants ********************************
250 DT = 1/200
260 TI = 0
270 DX = .0015
280 KO = 204
290 CP = 896
300 RHO = 2707
310 ALPHA = KO/(RHO*CP)
320 A = .0001
330 THETA = DT*ALPHA/DX2
340 PHI = DX*41860/KO
350 REM ************** start computation ***************************
360 OPEN "I",1,FILE$
370 OPEN "O",2,FILE2$
380 PRINT"RUNNING OUT OF FILE ";FILE$
390 PRINT#2,"TEMP1","TEMP2","TEMP3","TEMP4","TEMP5","TIME"
400 FOR M = 1 TO N
410 TI = TI + DT
420 IF EOF(1) THEN GOTO 460
430 INPUT#1,Q
440 IF Q<2 GOTO 420
450 GOTO 470
460 Q = 0
470 T(1) = T(1) + THETA*(T(2)-T(1)+Q*PHI)
480 FOR K = 2 TO 99
490 T(K) = T(K) + THETA*(T(K+1) - 2*T(K) + T(K-1))
500 NEXT K
510 T(100) = T(100) + THETA*(T(99)-T(100))
520 IF TI < R*.01 THEN GOTO 550
530 R = R + 1
540 PRINT#2,T(1),T(25),T(50),T(75),T(100),TI
550 NEXT M
560 CLOSE#1
570 CLOSE#2
580 PRINT "End Run. Output in file ";FILE2$
590 CLS
600 NEXT J
610 STOP
```

No of Copies	Organization
1	Office of the Secretary of Defense OUSD(A) Director, Live Fire Testing ATTN: James F. O'Bryon Washington, DC 20301-3110
2	Administrator Defense Technical Info Center ATTN: DTIC-DDA Cameron Station Alexandria, VA 22304-6145
1	HQDA (SARD-TR) WASH DC 20310-0001
1	Commander US Army Materiel Command ATTN: AMCDRA-ST 5001 Eisenhower Avenue Alexandria, VA 22333-0001
1	Commander US Army Laboratory Command ATTN: AMSLC-DL Adelphi, MD 20783-1145
2	Commander US Army, ARDEC ATTN: SMCAR-IMI-I Picatinny Arsenal, NJ 07806-5000
2	Commander US Army, ARDEC ATTN: SMCAR-TDC Picatinny Arsenal, NJ 07806-5000
1	Director Benet Weapons Laboratory US Army, ARDEC ATTN: SMCAR-CCB-TL Watervliet, NY 12189-4050
1	Commander US Army Armament, Munitions and Chemical Command ATTN: SMCAR-ESP-L Rock Island, IL 61299-5000
1	Commander US Army Aviation Systems Command ATTN: AMSAV-DACL 4300 Goodfellow Blvd. St. Louis, MO 63120-1798

No of Copies	Organization
1	Director US Army Aviation Research and Technology Activity ATTN: SAVRT-R (Library) M/S 219-3 Ames Research Center Moffett Field, CA 94035-1000
1	Commander US Army Missile Command ATTN: AMSMI-RD-CS-R (DOC) Redstone Arsenal, AL 35898-5010
1	Commander US Army Tank-Automotive Command ATTN: AMSTA-TSL (Technical Library) Warren, MI 48397-5000
1	Director US Army TRADOC Analysis Command ATTN: ATAA-SL White Sands Missile Range, NM 88002-5502
(Class. only)1	Commandant US Army Infantry School ATTN: ATSH-CD (Security Mgr.) Fort Benning, GA 31905-5660
(Unclass. only)1	Commandant US Army Infantry School ATTN: ATSH-CD-CSO-OR Fort Benning, GA 31905-5660
1	Air Force Armament Laboratory ATTN: AFATL/DLODL Eglin AFB, FL 32542-5000
	Aberdeen Proving Ground
2	Dir, USAMSAA ATTN: AMXSY-D AMXSY-MP, H. Cohen
1	Cdr, USATECOM ATTN: AMSTE-TD
3	Cdr, CRDEC, AMCCOM ATTN: SMCCR-RSP-A SMCCR-MU SMCCR-MSI
1	Dir, VLAMO ATTN: AMSLC-VL-D

No. of Copies	Organization
4	Director Defense Nuclear Agency ATTN: TDTR, CPT J. Hrinishin T.E. Kennedy SPWE, M.V. Oxford Shock Physics Directorate Washington, DC 20305-1000
1	Director Defense Nuclear Agency Test Directorate ATTN: CPT G. Brumburgh Kirtland AFB, NM 87115
1	Director Defense Nuclear Agency ATTN: TDTT, CPT J. Smith Kirtland AFB, NM 87115-5000
3	Director US Army Harry Diamond Laboratories ATTN: SLCHD-NW-TN, B. Schallhorn E. Fioravante A. Baba 2800 Powder Mill Road Adelphi, MD 20783-1197
4	Science Applications International Corporation ATTN: J. Simmons J. Guest J. Dishon P. Versteegen P.O. Box 1303 1710 Goodrich Drive McLean, VA 22102
1	AFIT/ENA ATTN: Prof. K. Matthews Wright-Patterson AFB, OH 45433-6583

No. of Copies	Organization

USER EVALUATION SHEET/CHANGE OF ADDRESS

This Laboratory undertakes a continuing effort to improve the quality of the reports it publishes. Your comments/answers to the items/questions below will aid us in our efforts.

1. BRL Report Number BRL-TR-3148 Date of Report SEPTEMBER 1990

2. Date Report Received _____

3. Does this report satisfy a need? (Comment on purpose, related project, or other area of interest for which the report will be used.) _____

4. Specifically, how is the report being used? (Information source, design data, procedure, source of ideas, etc.) _____

5. Has the information in this report led to any quantitative savings as far as man-hours or dollars saved, operating costs avoided, or efficiencies achieved, etc? If so, please elaborate. _____

6. General Comments. What do you think should be changed to improve future reports? (Indicate changes to organization, technical content, format, etc.) _____

CURRENT ADDRESS

Name

Organization

Address

City, State, Zip Code

7. If indicating a Change of Address or Address Correction, please provide the New or Correct Address in Block 6 above and the Old or Incorrect address below.

OLD ADDRESS

Name

Organization

Address

City, State, Zip Code

(Remove this sheet, fold as indicated, staple or tape closed, and mail.)